

# Regeneration of Light-Harvesting Complexes via Dynamic Replacement of Photodegraded Chromophores

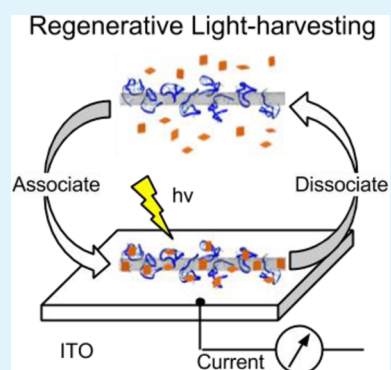
Hanyu Zhang,<sup>†</sup> Jing Pan,<sup>†</sup> Srijana Ghimire,<sup>‡</sup> Matthew A. Bork,<sup>‡</sup> Molly M. Riccitelli,<sup>†</sup> David R. McMillin,<sup>‡</sup> and Jong Hyun Choi<sup>\*,†</sup>

<sup>†</sup>School of Mechanical Engineering and <sup>‡</sup>Department of Chemistry, Purdue University, West Lafayette, Indiana 47907, United States

## Supporting Information

**ABSTRACT:** All-synthetic molecular donor–acceptor complexes are designed, which are capable of counteracting the effect of photoinduced degradation of donor chromophores. Anionic gallium protoporphyrin IX (GaPP) and semiconducting carbon nanotube (CNT) are used as a model donor–acceptor complex, which is assembled using DNA oligonucleotides. The GaPP-DNA-CNT complex produces an anodic photocurrent in a photoelectrochemical cell, which steadily decays due to photo-oxidation. By modulating the chemical environment, we showed that the photodegraded chromophores may be dissociated from the complex, whereas the DNA-coated carbon nanotube acceptors are kept intact. Reassociation with fresh porphyrins leads to the full recovery of GaPP absorption and photocurrents. This strategy could form a basis for improving the light-harvesting performance of molecular donor–acceptor complexes and extending their operation lifetime.

**KEYWORDS:** carbon nanotubes, porphyrin, donor–acceptor complex, photoelectrochemistry, photocurrent



Molecular light-harvesting complexes in natural photosystems are intricately arranged proteins and pigments that help collect sunlight in a photosynthetic reaction center where charge separation and electron transfer reactions take place. Inspired by such remarkable molecular machineries in nature, all-synthetic light-harvesting donor–acceptor complexes have been synthesized and studied extensively for photoelectrochemical conversion. Gust and co-workers constructed a variety of molecular donor–acceptor complexes and investigated their optical and electrochemical properties.<sup>1,2</sup> They showed that donor and acceptor molecules can be precisely tuned such that intra/intermolecular charge transfer processes are facilitated.<sup>3</sup> A fraction of excitation energy was down-regulated to protect the complexes from excessive light exposure, mimicking the photoprotection mechanisms in nature.<sup>4,5</sup> Numerous other research groups synthesized and studied various donor–acceptor complexes with novel photoelectrochemical properties, working toward artificial photosynthesis.<sup>6–8</sup>

Despite the recent advances in creating novel photoelectrochemical complexes and understanding the relevant charge transfer characteristics, the photostability remains one of the most critical issues in engineering the donor–acceptor pairs for solar energy utilization. In particular, photoinduced degradation of donor chromophores is prevalent such that conversion efficiency deteriorates over time. For example, porphyrin chromophores, widely used donor molecules, may degrade when photoinduced energy transfer from the chromophore to molecular oxygen in solution generates reactive oxygen species that can attack and oxidize the

molecules.<sup>9–11</sup> A strategy that can prevent or alleviate such inevitable adverse photoeffects would bolster donor–acceptor complexes as viable solar energy-harvesting materials as well as novel platforms to study charge transfer processes.<sup>12</sup> In this study, we demonstrate all-synthetic light-harvesting molecular donor–acceptor complexes capable of counteracting photoinduced degradation. To demonstrate this concept, we develop a facile oligonucleotide-based assembly strategy that allows us to exchange photodamaged donor molecules, while acceptors remain intact in a photoelectrochemical cell. The photoinduced decay of photocurrents is recovered (Figure 1a). This strategy could form a basis for improving overall system performance and service lifetime of donor–acceptor complexes for light harvesting.

In this work, we use anionic gallium(III) protoporphyrin IX chloride or GaPP (Figure 1b) and high-purity semiconducting single-wall carbon nanotubes as a model of molecular donors and acceptors. We use modified 30-mer oligonucleotide strands, originally identified via an *in vitro* selection process for selectively binding hemin or iron(III) protoporphyrin IX chloride (FePP), which has the same molecular structure as GaPP except for a change of the metal cation.<sup>13</sup> We demonstrate that photobleached porphyrins can be dissociated from DNA-coated carbon nanotubes immobilized on an indium tin oxide (ITO) surface, and that the photocurrents fully recover after fresh GaPP molecules are reintroduced to the

Received: March 3, 2015

Accepted: April 6, 2015

Published: April 7, 2015



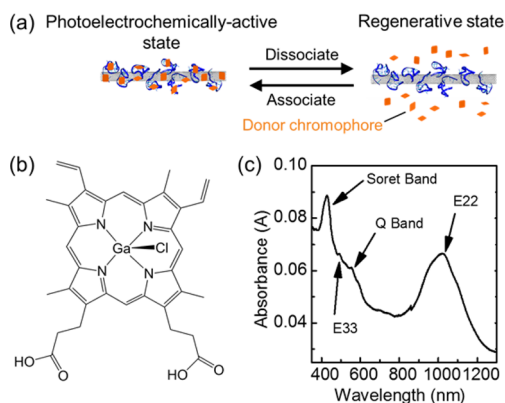


**Figure 1.** (a) Schematic of a light-harvesting photoelectrochemically active system compatible with dissociating and associating donor chromophores. (b) Gallium(III) protoporphyrin IX chloride (GaPP). (c) Absorption spectrum of GaPP-DNA-CNT complex film showing prominent features of Soret band of the porphyrin chromophore and the  $E_{22}$  transition of semiconducting single-wall carbon nanotubes.

system for reassociation. Four successive regenerations result in a 50% increase in the overall photoconversion efficiency within a 90 min illumination period compared to a nonregenerated system.

The light-harvesting donor–acceptor complex samples are prepared by depositing DNA-dispersed carbon nanotubes in aqueous solution on a membrane using a vacuum filtration system, followed by transferring them onto an ITO substrate and immersing the transferred sample in a GaPP-containing solution for 1 h (see Experimental Methods in the Supporting Information for details). The 30-mer single-stranded DNA oligonucleotides (T12PS2M or 5′-T<sub>12</sub>GTG<sub>3</sub>TAG<sub>3</sub>CG<sub>3</sub>TTGG-3′) are used for noncovalently linking GaPP, while dispersing nanotubes in aqueous solution. The guanine (G)-rich part of the DNA strand forms a G-quadruplex conformation, facilitating target porphyrin recognition, whereas the 5′-T<sub>12</sub> leader sequence is designed to adhere to the nanotube surface.<sup>14</sup> The absorption spectrum of the deposited GaPP-DNA-CNT film on the ITO substrate is shown in Figure 1c. Here, two prominent features are observed. The Soret band of GaPP is found at ~410 nm, whereas the peak around 1000 nm arises from the electronic transition between the second van Hove singularities (the so-called  $E_{22}$ ) of the semiconducting single-wall carbon nanotubes.<sup>15,16</sup> Minor signatures such as Q-band of GaPP and  $E_{33}$  of carbon nanotubes are also present, albeit weak, between 450 and 600 nm. Resonant Raman scattering shows a minimal disorder mode (D peak) at approximately 1350  $\text{cm}^{-1}$  (Figure S1 in the Supporting Information), suggesting that the noncovalent interaction of DNA with the nanotube surface does not disturb the electronic band structure of the nanotubes significantly. Two-dimensional Raman contour map and atomic force microscope (AFM) image indicate that the deposited complex film is percolated carbon nanotube network with an average thickness of roughly 10 nm (Figure S2 and S3 in the Supporting Information).

The use of the GaPP-DNA-CNT complexes for photocurrent generation was examined in a photoelectrochemical cell using 150 mM ferrocyanide ( $\text{Fe}(\text{CN})_6^{4-}$ ) and 150 mM ferricyanide ( $\text{Fe}(\text{CN})_6^{3-}$ ) as a redox couple. Figure 2a shows that the limiting photocurrent of approximately 6  $\mu\text{Amp}$  was measured from the complex sample containing 4  $\mu\text{g}$  of carbon nanotubes when the 350–700 nm light at ~400  $\text{mW}/\text{cm}^2$  was

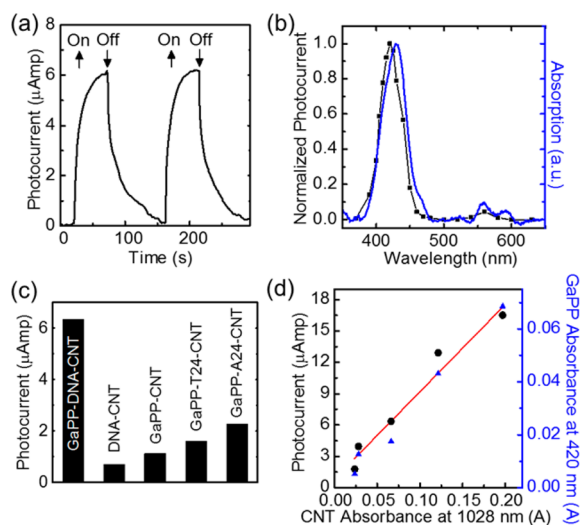


**Figure 2.** (a) Photocurrent generated by GaPP-DNA-CNT complexes. (b) Action spectrum of the complex. The black-dotted line indicates the normalized photocurrent collected under light illumination at the corresponding wavelengths; the absorption spectrum of the GaPP portion of the GaPP-DNA-CNT complexes with the SWCNT background subtracted. (c) Comparison of various samples including GaPP-DNA-CNT, DNA-CNT, GaPP-CNT, GaPP-T24-CNT, and GaPP-A24-CNT films. (d) Photocurrents at different amount of the GaPP-DNA-CNT complexes (black dots) along with the corresponding Soret band absorption of GaPP (~410 nm, blue dots).

turned on, and quickly diminished with the light off. The kinetics of the photocurrents in Figure 2a is attributed to  $\text{Fe}(\text{CN})_6^{3-/4-}$  as other redox couples such as ascorbate/dehydroascorbic acid under similar conditions demonstrates fast photocurrent activities in response to light irradiation (Figure S4 in the Supporting Information).<sup>17</sup> We found that ferrocyanide plays a more important role in the photocurrent generation than ferricyanide. We varied concentrations of ferricyanide/ferrocyanide while their total amount was fixed at 300 mM (Figure S5 in the Supporting Information). The photocurrents generated with 250 or 150 mM ferrocyanide were nearly identical at approximately 6.5  $\mu\text{Amp}$ , whereas only ~1  $\mu\text{Amp}$  was observed with 50 mM ferrocyanide. In these anodic photocurrent experiments, the electrons generated from the photoirradiated sample are collected at the ITO, the working electrode. Photoabsorption of GaPP chromophores leads to charge separation at the interface with carbon nanotubes.<sup>18,19</sup> The photogenerated electrons are transferred to the carbon nanotubes, which shuttle the electrons to the working electrode.<sup>20</sup> The oxidized GaPP molecules are reduced by ferrocyanide in the electrolyte, which becomes an oxidizing product, ferricyanide. The ferricyanide molecules diffuse to the platinum counter electrode and become reduced to ferrocyanide, completing the entire photoelectrochemical circuit.<sup>17</sup>

The photoconversion process is confirmed by the action spectra in Figure 2b, where photocurrent and optical absorption are plotted as a function of irradiating wavelength from 350 to 650 nm. Both spectra are in excellent agreement with regard to GaPP signatures at ~410 nm (Soret) and between 550 and 600 nm (Q-band). This observation indicates that both singlet transitions ( $S_0 \rightarrow S_2$ : Soret and  $S_0 \rightarrow S_1$ : Q) can contribute to the transfer of photogenerated electrons to the carbon nanotube acceptor, whereas the electrons in the  $S_2$  state likely depopulate to the  $S_1$  state before charge injection

given their fast relaxation kinetics.<sup>21</sup> Similar charge transfer processes were reported previously with other porphyrin/carbon nanotube complex systems.<sup>22</sup>

The photocurrent of the GaPP-DNA-CNT film is compared with those of several control samples under identical conditions including the same amount of carbon nanotubes in the films (Figure 2c). The DNA-CNT film with no GaPP molecules barely demonstrate measurable photocurrents ( $\sim 0.5 \mu\text{Amp}$ ) as expected, consistent with GaPP chromophores being electron donors for this light-harvesting complex system.<sup>21,23</sup> The GaPP-CNT film fabricated without DNA strands also shows a small amount of photocurrent ( $\sim 1 \mu\text{Amp}$ ), consistent with its absorption spectrum indicating a minimal amount of GaPP chromophores (Figure S6 in the Supporting Information). Two control DNA sequences of 24-base-long consecutive poly thymine ( $T_{24}$ ) and poly adenine ( $A_{24}$ ) demonstrate photocurrents of approximately  $2 \mu\text{Amp}$ , about three times smaller than that of the GaPP-DNA-CNT film. Correspondingly, the optical absorption spectra of the control samples with  $T_{24}$  and  $A_{24}$  strands show reduced amounts of GaPP chromophores (Figure S6 in the Supporting Information). This result indicates that the ability of T12PS2M DNA for selective binding of GaPP is well-retained on the nanotubes, whereas nonspecific adsorption of anionic GaPP on the DNA-CNT film is less important.

The amount of light-harvesting complexes used in the film determines the resulting photocurrents. Figure 2d shows that the increased amount of DNA-functionalized carbon nanotubes (black circles) capture a greater number of GaPP molecules (blue triangles), resulting in an increasing photocurrent. The corresponding absorption spectra showing the Soret and  $E_{22}$  bands are presented in Figure S7 in the Supporting Information.

The photoelectrochemical properties of the donor–acceptor complexes are also a strong function of light-irradiation intensity as shown in Figure 3a. The rate of photocurrent decay was much faster at  $400 \text{ mW/cm}^2$  than at  $70 \text{ mW/cm}^2$ , which we attribute to a more rapid photoinduced degradation of the porphyrin chromophores. With light illumination and dissolved oxygen in the electrolyte, GaPP molecules experience photo-oxidation, leading to degradation and ultimately photocurrent decay of the complex film.<sup>9,24</sup> With the  $N_2$  purged

electrolyte, the GaPP-DNA-CNT complex film experienced a slower rate of decay, indicating that the degradation effect was relieved by reducing dissolved oxygen in the electrolyte (Figure S8 in the Supporting Information). This photodamage effect may also be counteracted by replacing photodegraded chromophores with fresh porphyrins. In Figure 3b, c, we show a series of optical absorption spectra and corresponding photocurrents recorded during the regeneration process. Initially, a DNA-coated CNT film (shown in black in Figure 3b, c) was characterized with no GaPP Soret signature and minimal current signals under illumination. This film was then incubated with a GaPP-containing solution to allow the DNA strands to interact with GaPP molecules, forming the light-harvesting complexes. The donor–acceptor system demonstrates a strong Soret feature and photocurrent (shown in red in Figure 3b, c). We then submerged the complex film in the 30 wt % hydrogen peroxide solution for 1 h to displace GaPP molecules. The proposed mechanism for the porphyrin dissociation is that  $H_2O_2$ -induced oxidation of GaPP results in the destruction of porphyrin rings and/or dissociation from the DNA strands.<sup>25,26</sup> The hydrogen peroxide-based treatment is found to be effective at removing the porphyrins, whereas carbon nanotubes were well-retained on the ITO as they show no apparent changes in their optical absorption. After the GaPP removal, the film may have some porphyrin residue as seen in absorption, but its contribution to photocurrents was trivial (shown in blue in Figure 3b, c). Finally, the film was refunctionalized with fresh donor chromophores by reassociation with porphyrins in a new solution. The absorption spectrum and photocurrent signal of the final GaPP-DNA-CNT complex film (shown in green in Figure 3b, c) are nearly identical with those of the original GaPP-DNA-CNT film (shown in red).

The results in Figure 3 also indicate that DNA–carbon nanotubes are intact after the  $H_2O_2$  treatment. No significant effects on the carbon nanotubes are expected in the  $H_2O_2$  treatment for 1 h without temperature elevation,<sup>27,28</sup> whereas their surface may be protonated at low pH and reversibly deprotonated at high pH.<sup>29</sup> To ascertain whether DNA strands remain intact after the treatment with 30 wt %  $H_2O_2$  solution, we performed a control experiment designed to damage DNA via the Fenton chemistry (Figure S9 in the Supporting Information). Here, a GaPP-DNA-CNT film was exposed to  $50 \mu\text{M}$  iron sulfate ( $FeSO_4$ ) in 100 mM  $H_2O_2$  solution for DNA cleavage after GaPP dissociation.<sup>30</sup> After the Fenton reaction, the film was washed thoroughly and the reassociation with GaPP was carried out. With the DNA damaged, the Soret band of the GaPP-DNA-CNT film was drastically lower at approximately 20% of the intact GaPP-DNA-CNT film as the damaged oligonucleotides were unable to anchor the GaPP.

Of considerable utility in our strategy is that the regeneration of donor chromophores can be repeated indefinitely. As proof-of-concept, we performed multiple regeneration cycles for a GaPP-DNA-CNT film, measured its photocurrent over time, and compared it with the film without porphyrin replacement (Figure 4). To facilitate photodegradation of the donor chromophores, we used high light intensity at  $\sim 400 \text{ mW/cm}^2$  on the sample. As shown in Figure 4, the complex film without regeneration demonstrates a continuous decay of photocurrent, quickly decreasing to 50% of its initial photocurrent signal within the first thousand seconds (black curve). Another donor–acceptor complex film was regenerated after 1000 s by replacing the photodamaged porphyrins through the  $H_2O_2$  treatment and

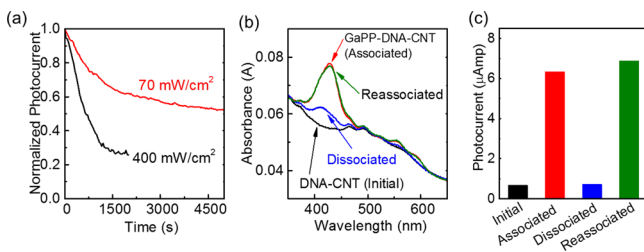


**Figure 3.** (a) Photocurrent decays of the GaPP-DNA-CNT complexes under light illumination at 70 and  $400 \text{ mW/cm}^2$ . (b) Absorption spectra and (c) corresponding photocurrents during the sequential regeneration process: (i) initial DNA-CNT film with no GaPP (black), (ii) the DNA-CNT film after association with GaPP (red), (iii) the GaPP-DNA-CNT film after GaPP dissociation (blue), and (iv) the GaPP-DNA-CNT film after reassociation with GaPP (green). A mixture solution of 150 mM ferricyanide and 150 mM ferrocyanide was used as the electrolyte. For photocurrent measurement in c, a xenon arc lamp was used and the light intensity at the sample was measured at  $\sim 400 \text{ mW/cm}^2$ .

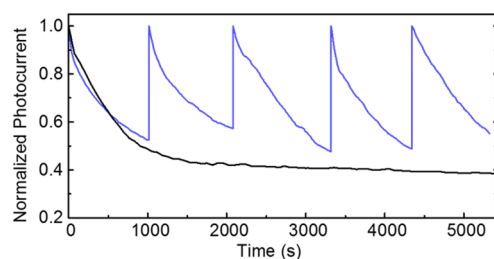


**Figure 4.** Photocurrent of the GaPP-DNA-CNT complexes produced through four regeneration events (blue) and that of the complexes without regeneration (black). With four regeneration events, the overall conversion efficiency increases by 50% within the 90 min irradiation period compared with the sample without regeneration. A mixture of ferrocyanide (150 mM) and ferricyanide (10 mM) was as the electrolyte for the photocurrent measurement.

association with fresh porphyrins as described above. Such regeneration was repeated four times (blue curve). During the 90 min irradiation period, the overall photocurrent efficiency increased by 50% compared with the sample without regeneration. We expect that for a 24 h illumination period, the regenerated system would achieve 16 times more photocurrent output than the film without replacement of photodegraded chromophores. This novel approach may be potentially used for improving overall performance of donor–acceptor complexes and dramatically extending their light-harvesting service lifetime.

In this Letter, we demonstrate a novel strategy that counteracts the photodegradation in all-synthetic molecular donor–acceptor complexes for light harvesting. Gallium protoporphyrins and semiconducting carbon nanotubes, the model donors and acceptors in this study, are assembled by using 30-mer oligonucleotides that have a strong affinity for the protoporphyrins. This complex demonstrates a consistent anodic photocurrent, originated from optical absorption of the porphyrin chromophores, followed by the excited-state electron transfer to carbon nanotubes on the ITO working electrode. The complex shows a superior ability for light harvesting and conversion compared to other samples without the porphyrins and based on other DNA sequences. Photo-induced degradation of the donor chromophores results in the decay of photocurrents over time. The regeneration of the complex film was demonstrated by sequentially dissociating the damaged donors from the complex and associating with fresh porphyrins, whereas the DNA-coated carbon nanotube acceptors were kept intact. The photocurrent recovered fully when the complex film was regenerated. Compared with the sample without regeneration, a 50% increase in photocurrent was observed from four repeated regeneration cycles within a 90 min irradiation period. The bioinspired approach of dynamically replacing photodegraded chromophores in the donor–acceptor complex could form a basis for solar energy-harvesting systems with drastically improved overall performance and extended service lifetime.

## ■ ASSOCIATED CONTENT

### Supporting Information

Experimental section, optical absorption, Raman spectra, and photoelectrochemical measurements. This material is available free of charge via the Internet at <http://pubs.acs.org>.

## ■ AUTHOR INFORMATION

### Corresponding Author

\* Email: [jchoi@purdue.edu](mailto:jchoi@purdue.edu).

### Notes

The authors declare no competing financial interest.

## ■ ACKNOWLEDGMENTS

The authors acknowledge support from the National Science Foundation.

## ■ REFERENCES

- (1) Sherman, B. D.; Vaughn, M. D.; Bergkamp, J. J.; Gust, D.; Moore, A. L.; Moore, T. A. Evolution of Reaction Center Mimics to Systems Capable of Generating Solar Fuel. *Photosynth. Res.* **2014**, *120*, 59–70.
- (2) Gust, D.; Moore, T. A.; Moore, A. L. Realizing Artificial Photosynthesis. *Faraday Discuss.* **2012**, *155*, 9–26.
- (3) Gust, D.; Moore, T. A.; Moore, A. L. Mimicking Photosynthetic Solar Energy Transduction. *Acc. Chem. Res.* **2001**, *34*, 40–48.
- (4) Straight, S. D.; Kodis, G.; Terazono, Y.; Hambourger, M.; Moore, T. A.; Moore, A. L.; Gust, D. Self-Regulation of Photoinduced Electron Transfer by a Molecular Nonlinear Transducer. *Nat. Nanotechnol.* **2008**, *3*, 280–283.
- (5) Megiatto, J. D.; Antoniuk-Pablant, A.; Sherman, B. D.; Kodis, G.; Gervald, M.; Moore, T. A.; Moore, A. L.; Gust, D. Mimicking the Electron Transfer Chain in Photosystem II with a Molecular Triad Thermodynamically Capable of Water Oxidation. *Proc. Natl. Acad. Sci. U.S.A.* **2012**, *109*, 15578–15583.
- (6) Tachibana, Y.; Vayssieres, L.; Durrant, J. R. Artificial Photosynthesis for Solar Water-Splitting. *Nat. Photonics* **2012**, *6*, 511–518.
- (7) Colvin, M. T.; Ricks, A. B.; Scott, A. M.; Smeigh, A. L.; Carmieli, R.; Miura, T.; Wasielewski, M. R. Magnetic Field-Induced Switching of the Radical-Pair Intersystem Crossing Mechanism in a Donor-Bridge-Acceptor Molecule for Artificial Photosynthesis. *J. Am. Chem. Soc.* **2010**, *133*, 1240–1243.
- (8) Kloz, M.; Pillai, S.; Kodis, G.; Gust, D.; Moore, T. A.; Moore, A. L.; van Grondelle, R.; Kennis, J. T. New Light-Harvesting Roles of Hot and Forbidden Carotenoid States in Artificial Photosynthetic Constructs. *Chem. Sci.* **2012**, *3*, 2052–2061.
- (9) Krieg, M.; Whitten, D. G. Self-Sensitized Photo-Oxidation of Protoporphyrin IX and Related Porphyrins in Erythrocyte Ghosts and Microemulsions: a Novel Photo-Oxidation Pathway Involving Singlet Oxygen. *J. Photochem.* **1984**, *25*, 235–252.
- (10) Bezdetnaya, L.; Zeghari, N.; Bulitchenko, I.; Barberl-Heyob, M.; Merlin, J. L.; Potapenko, A.; Gullemin, F. Spectroscopic and Biological Testing of Photobleaching of Porphyrins in Solutions. *Photochem. Photobiol.* **1996**, *64*, 382–386.
- (11) Moan, J.; BERG, K. The Photodegradation of Porphyrins in Cells can be Used to Estimate the Lifetime of Singlet Oxygen. *Photochem. Photobiol.* **1991**, *53*, 549–553.
- (12) Ham, M.-H.; Choi, J. H.; Boghossian, A. A.; Jeng, E. S.; Graff, R. A.; Heller, D. A.; Chang, A. C.; Mattis, A.; Bayburt, T. H.; Grinkova, Y. V. Photoelectrochemical Complexes for Solar Energy Conversion that Chemically and Autonomously Regenerate. *Nat. Chem.* **2010**, *2*, 929–936.
- (13) Li, Y.; Geyer, R.; Sen, D. Recognition of Anionic Porphyrins by DNA Aptamers. *Biochemistry* **1996**, *35*, 6911–6922.
- (14) Zheng, M.; Jagota, A.; Semke, E. D.; Diner, B. A.; McLean, R. S.; Lustig, S. R.; Richardson, R. E.; Tassi, N. G. DNA-Assisted Dispersion and Separation of Carbon Nanotubes. *Nat. Mater.* **2003**, *2*, 338–342.
- (15) Jackson, R. K.; Munro, A.; Nebesny, K.; Armstrong, N.; Graham, S. Evaluation of Transparent Carbon Nanotube Networks of Homogeneous Electronic Type. *ACS Nano* **2010**, *4*, 1377–1384.
- (16) Wójtowicz, H.; Bielecki, M.; Wojaczyński, J.; Olczak, M.; Smalley, J. W.; Olczak, T. The Porphyrinomonas Gingivalis HmuY Haemophore Binds Gallium (III), Zinc (II), Cobalt (III), Manganese (III), Nickel (II), and Copper (II) Protoporphyrin IX but in a Manner

Different to Iron (III) Protoporphyrin IX. *Metallomics* **2013**, *5*, 343–351.

(17) Calkins, J. O.; Umasankar, Y.; O'Neill, H.; Ramasamy, R. P. High Photo-Electrochemical Activity of Thylakoid-Carbon Nanotube Composites for Photosynthetic Energy Conversion. *Energy Environ. Sci.* **2013**, *6*, 1891–1900.

(18) D'Souza, F.; Das, S. K.; Zandler, M. E.; Sandanayaka, A. S.; Ito, O. Bionano Donor-Acceptor Hybrids of Porphyrin, ssDNA, and Semiconductive Single-Wall Carbon Nanotubes for Electron Transfer via Porphyrin Excitation. *J. Am. Chem. Soc.* **2011**, *133*, 19922–19930.

(19) Romero-Nieto, C.; García, R.; Herranz, M. A.; Ehli, C.; Ruppert, M.; Hirsch, A.; Guldi, D. M.; Martín, N. Tetrathiafulvalene-Based Nanotweezers-Noncovalent Binding of Carbon Nanotubes in Aqueous Media with Charge Transfer Implications. *J. Am. Chem. Soc.* **2012**, *134*, 9183–9192.

(20) Guldi, D. M.; Rahman, G.; Prato, M.; Jux, N.; Qin, S.; Ford, W. Single-Wall Carbon Nanotubes as Integrative Building Blocks for Solar-Energy Conversion. *Angew. Chem.* **2005**, *117*, 2051–2054.

(21) Zhang, H.; Bork, M. A.; Riedy, K. J.; McMillin, D. R.; Choi, J. H. Understanding Photophysical Interactions of Semiconducting Carbon Nanotubes with Porphyrin Chromophores. *J. Phys. Chem. C* **2014**, *118*, 11612–11619.

(22) Rahman, G. A.; Guldi, D. M.; Campidelli, S.; Prato, M. Electronically Interacting Single Wall Carbon Nanotube-Porphyrin Nanohybrids. *J. Mater. Chem.* **2006**, *16*, 62–65.

(23) Zhang, H.; Baker, B. A.; Cha, T. G.; Sauffer, M. D.; Wu, Y.; Hinkson, N.; Bork, M. A.; McShane, C. M.; Choi, K. S.; McMillin, D. R. DNA Oligonucleotide Templated Nanohybrids Using Electronic Type Sorted Carbon Nanotubes for Light Harvesting. *Adv. Mater.* **2012**, *24*, 5447–5451.

(24) Cox, G. S.; Bobillier, C.; Whitten, D. G. Photooxidation and Singlet Oxygen Sensitization by Protoporphyrin IX and its Photooxidation Products. *Photochem. Photobiol.* **1982**, *36*, 401–407.

(25) Travascio, P.; Li, Y.; Sen, D. DNA-Enhanced Peroxidase Activity of a DNA Aptamer-Hemin Complex. *Chem. Biol.* **1998**, *5*, 505–517.

(26) George, P.; Irvine, D. The Reaction Between Metmyoglobin and Hydrogen Peroxide. *Biochem. J.* **1952**, *52*, 511–517.

(27) Miyata, Y.; Maniwa, Y.; Kataura, H. Selective Oxidation of Semiconducting Single-Wall Carbon Nanotubes by Hydrogen Peroxide. *J. Phys. Chem. B* **2005**, *110*, 25–29.

(28) Ellison, M. D.; Buckley, L. K.; Lewis, G. G.; Smith, C. E.; Siedlecka, E. M.; Palchak, C. V.; Malarchik, J. M. Photochemical Hydroboration-Oxidation of Single-Walled Carbon Nanotubes. *J. Phys. Chem. C* **2009**, *113*, 18536–18541.

(29) Strano, M. S.; Huffman, C. B.; Moore, V. C.; O'Connell, M. J.; Haroz, E. H.; Hubbard, J.; Miller, M.; Rialon, K.; Kittrell, C.; Ramesh, S.; Hauge, R. H.; Smalley, R. E. Reversible, Band-Gap-Selective Protonation of Single-Walled Carbon Nanotubes in Solution. *J. Phys. Chem. B* **2003**, *107*, 6979–6985.

(30) Imlay, J. A.; Linn, S. DNA Damage and Oxygen Radical Toxicity. *Science* **1988**, *240*, 1302–1309.